Supplementary Information

Dose-Fractionated Electron Ptychography for Atomic-Resolution Imaging Under Ultra-Low Dose

Xudong Pei, Yu Lei et al.

Supplementary Figures

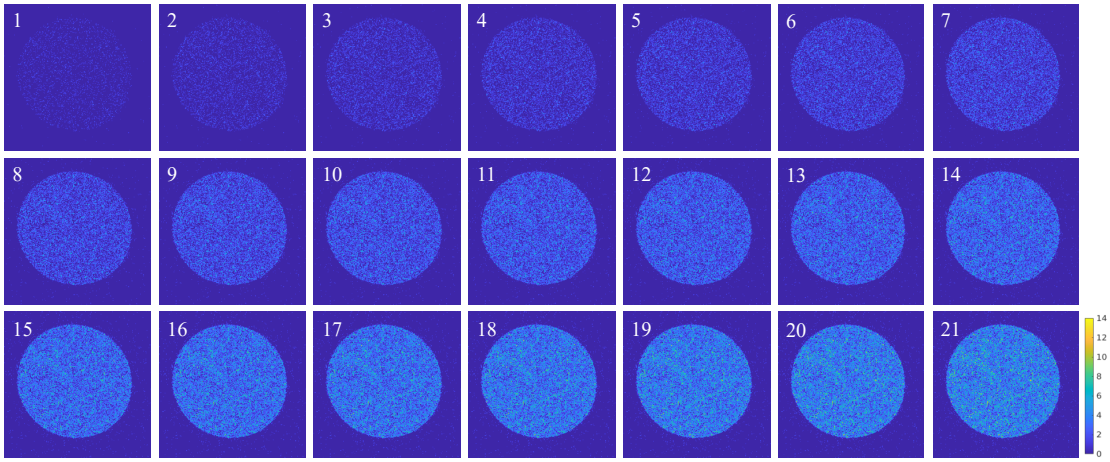

Supplementary Fig. 1

Typical integrated diffraction patterns at a single scan position, obtained by summing 1-21 sub-frames from the 5D dataset. Increased frame number leads to improved signal-to-noise ratio and reveals higher-frequency features in the diffraction pattern. All patterns are shown with identical intensity scaling for direct comparison.

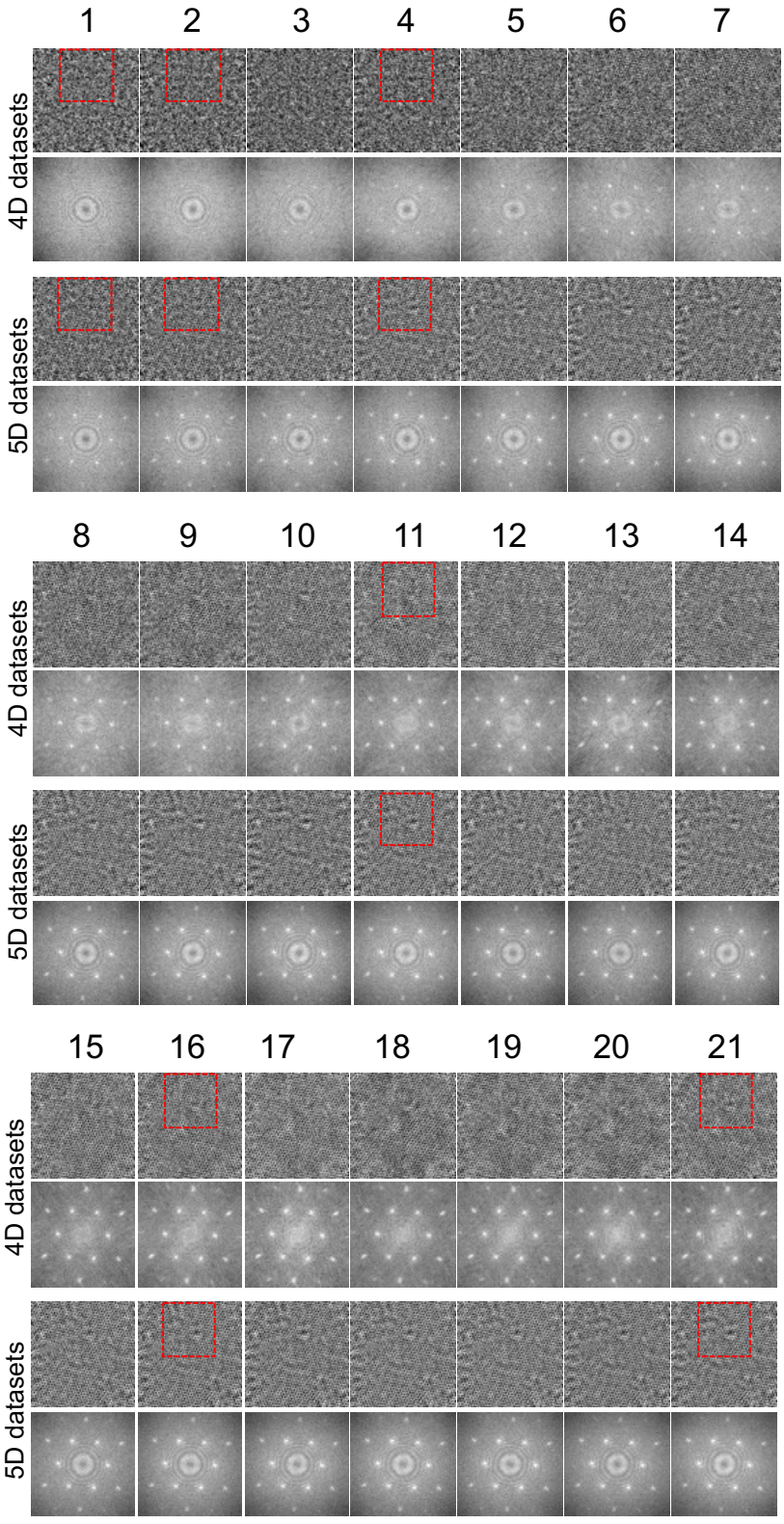

Supplementary Fig. 2

Comparison of ptychographic reconstructions and corresponding power spectra from integrated 4D datasets and 5D datasets for varying numbers of sub-frames (1–21).

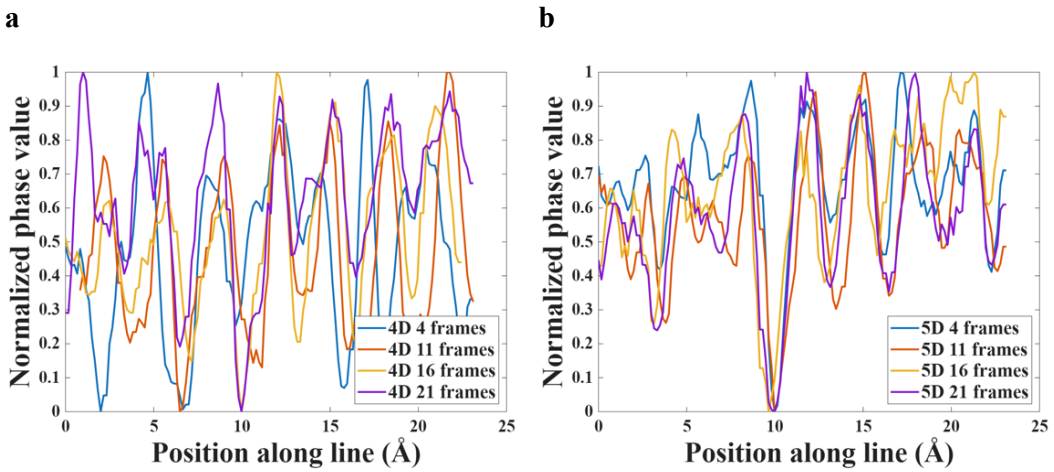

Supplementary Fig. 3

Line profiles (across red line in Fig.2) of a sulfur atom defect extracted from phase images reconstructed using (a) integrated 4D datasets and (b) dose-fractionated 5D datasets with 4, 11, 16, and 21 sub-frames per illumination position.

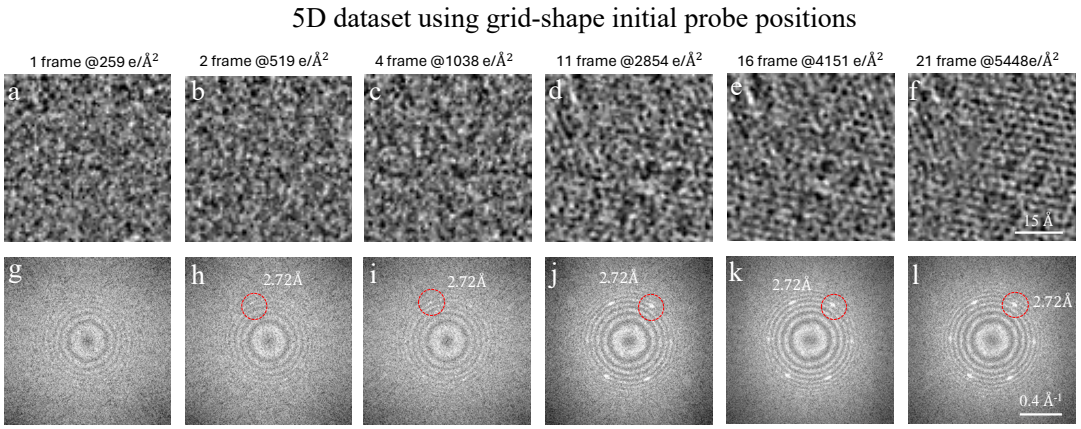

Supplementary Fig. 4

Reconstructed phase images (top row) and corresponding power spectra (bottom row) obtained by directly assigning nominal grid-shaped probe positions to dose-fractionated 5D datasets comprising 1, 2, 4, 11, 16, and 21 frames per illumination position. The total electron doses for these datasets are 260 e/Å², 519 e/Å², 1038 e/Å², 2854 e/Å², 4151 e/Å², and 5448 e/Å², respectively.

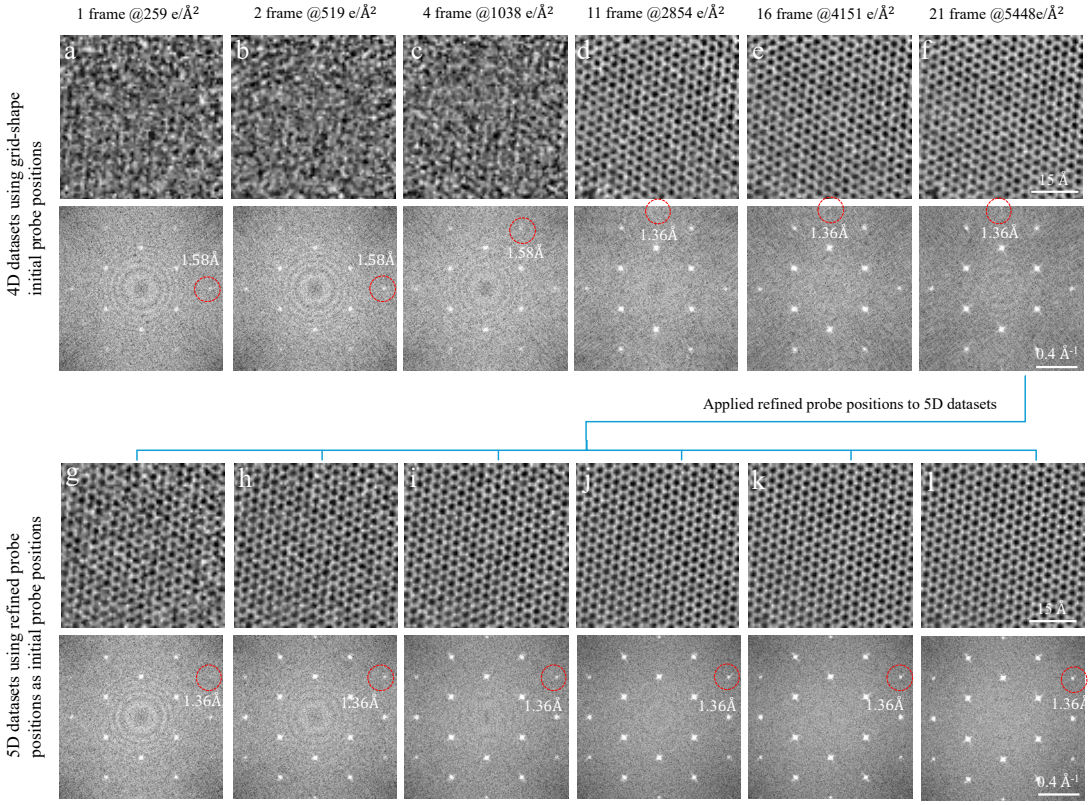

Supplementary Fig. 5

Simulated ptychographic phase reconstructions corresponding to the experimental results in Fig. 2. Top row (a – f): phase reconstructions and their power spectra from integrated 4D datasets simulated with 1, 2, 4, 11, 16, and 21 sub-frames per illumination position. Bottom row (g – l): corresponding reconstructions and power spectra from 5D datasets with the same frame numbers. Simulations were performed using a monolayer MoS_2 model under identical optical parameters, dose conditions, and refined probe positions as in the experiments, with reconstructions carried out using the same workflow. The details of simulation are provided in Supplementary Note 1. These results further demonstrate resolution enhancement achieved through data-driven correction of inter-frame shifts.

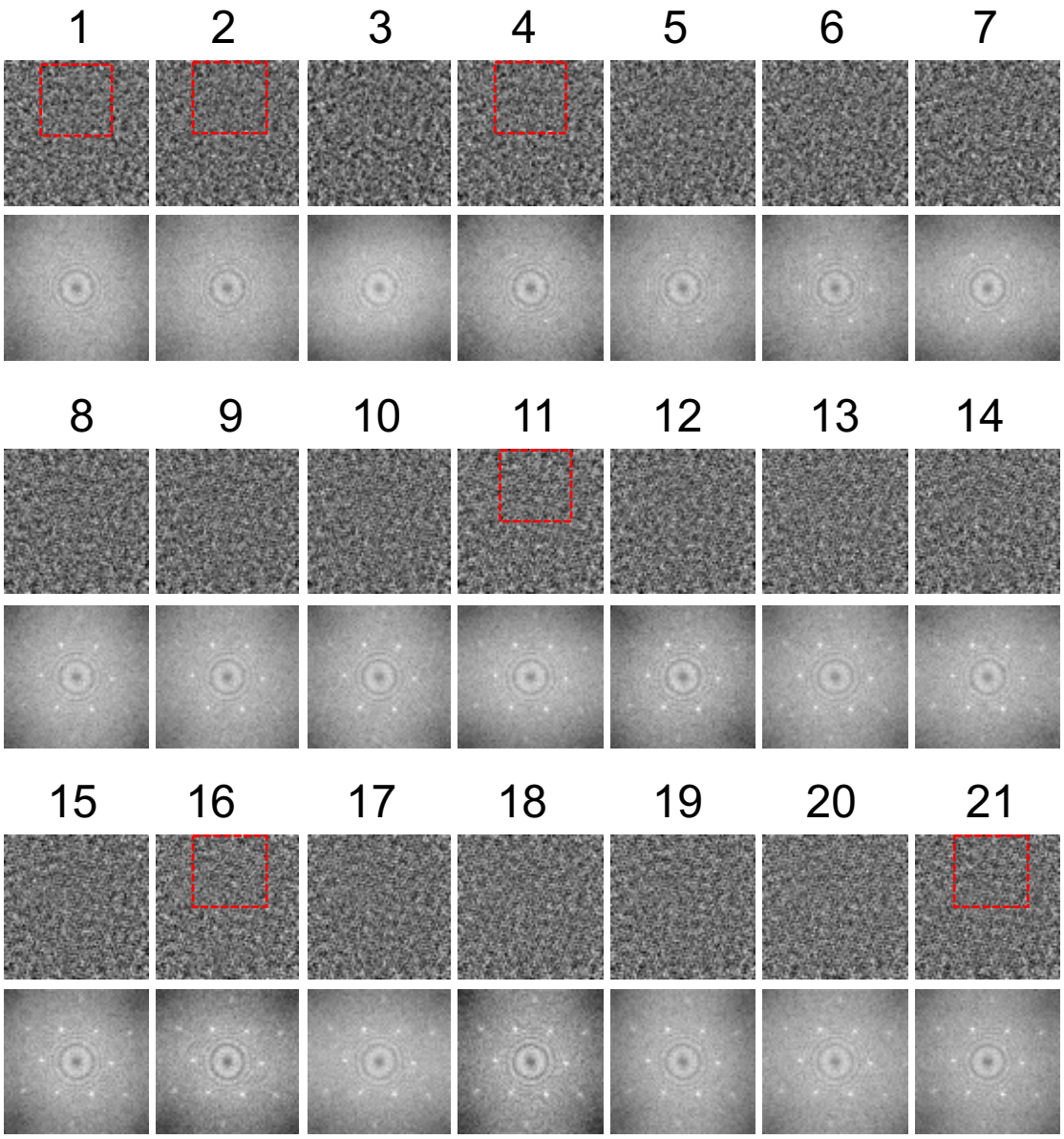

Supplementary Fig. 6

Comparison of ptychographic reconstructions on the same 4D dataset using different initial positions derived from integrated datasets with varying numbers of sub-frame (1 – 21).

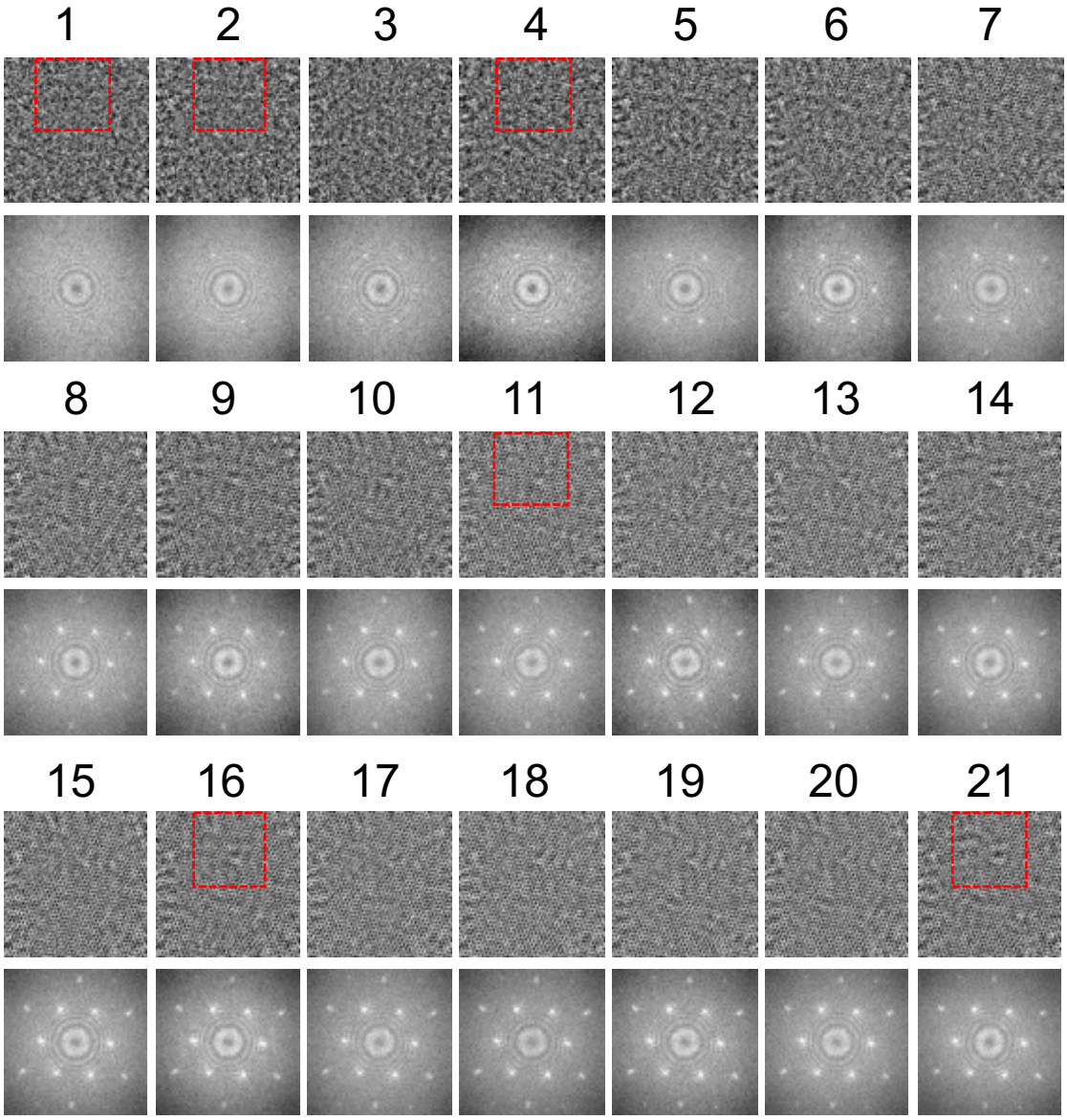

Supplementary Fig. 7

Comparison of ptychographic reconstructions on the 5D datasets themself used to drive position refinement, using initial positions derived from integrated datasets with varying frame numbers (1 – 21).

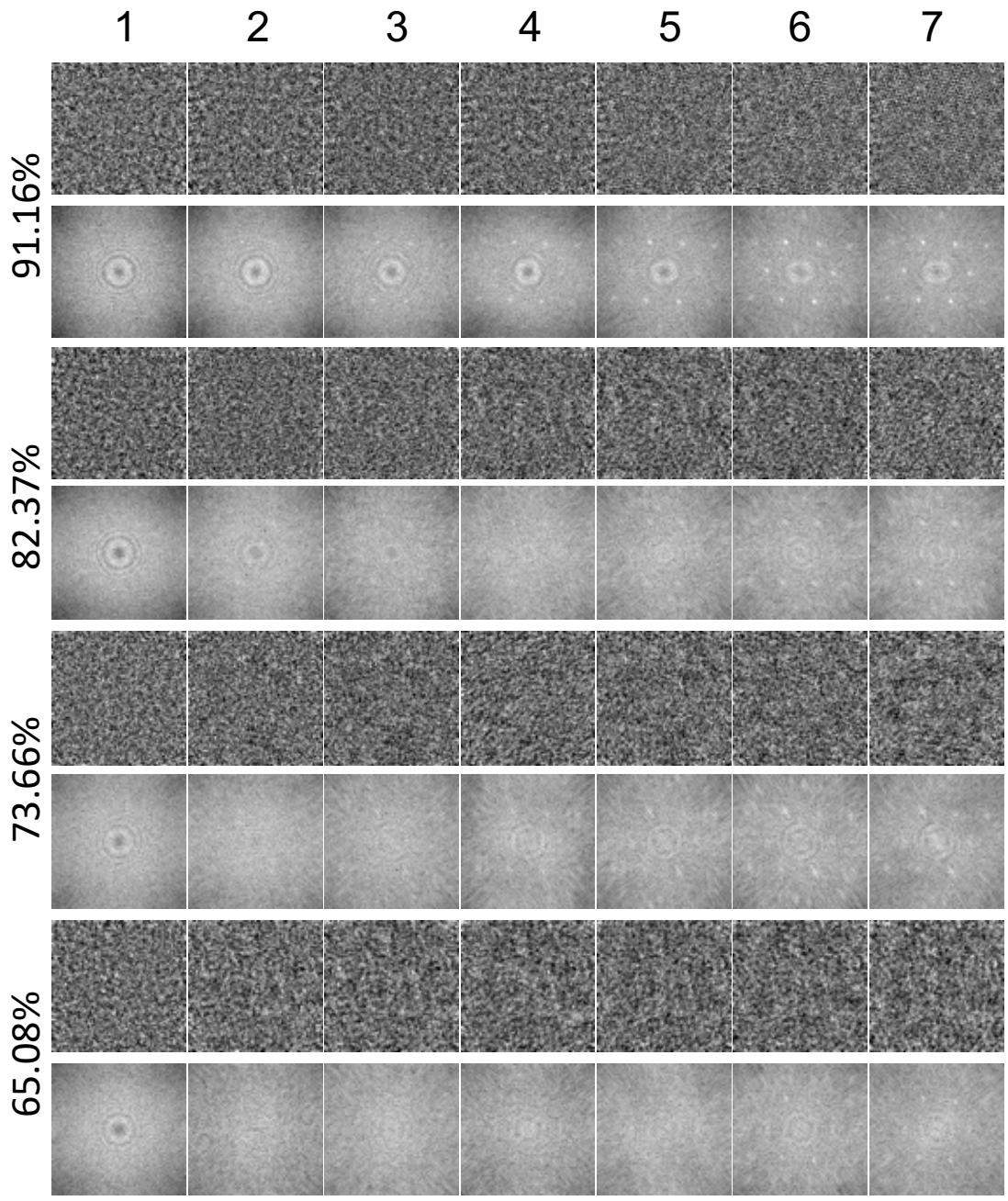
1
2
3
4
5
6
7
91.16%
82.37%
73.66%
65.08%

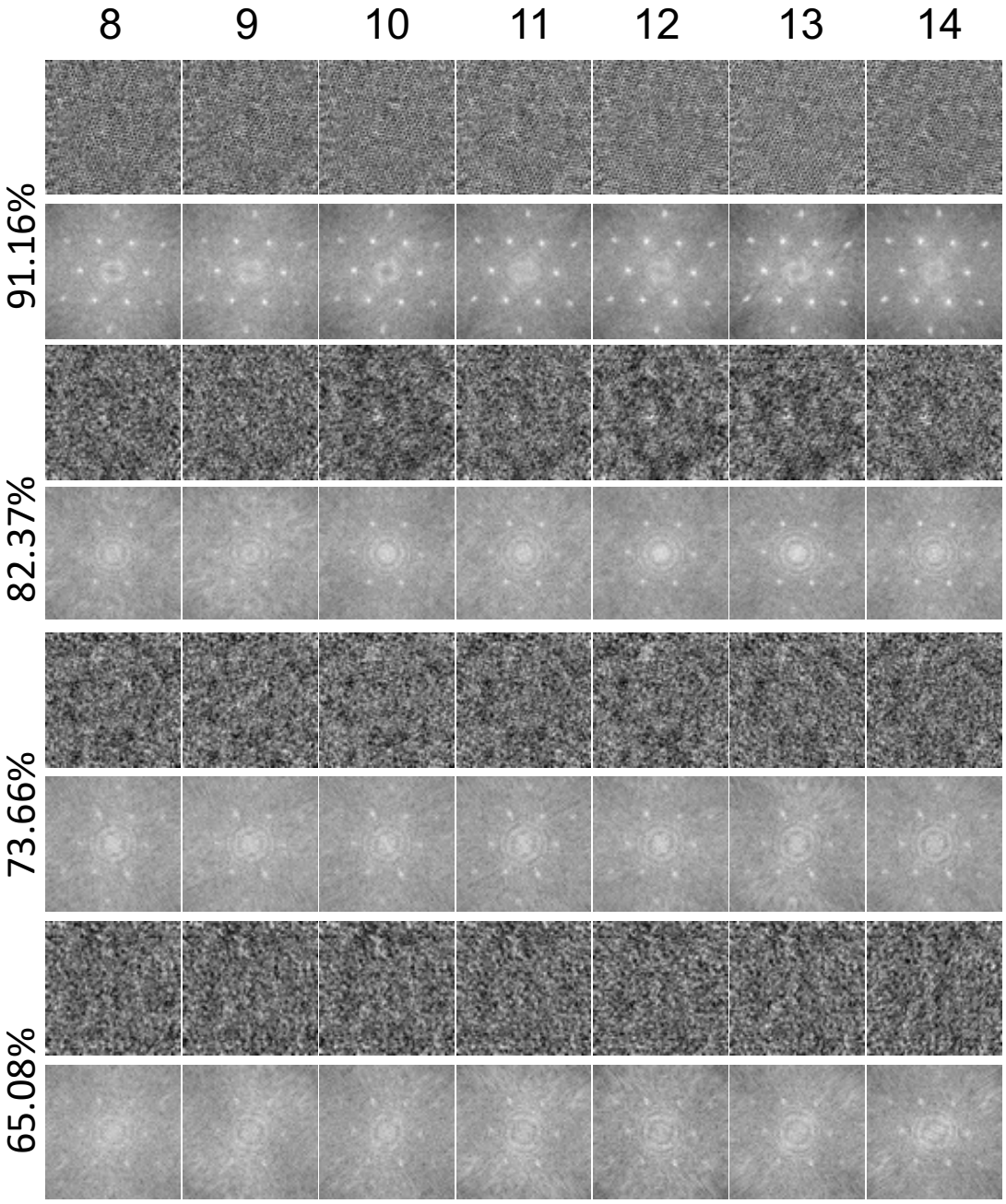
8
9
10
11
12
13
14
91.16%
82.37%
73.66%
65.08%

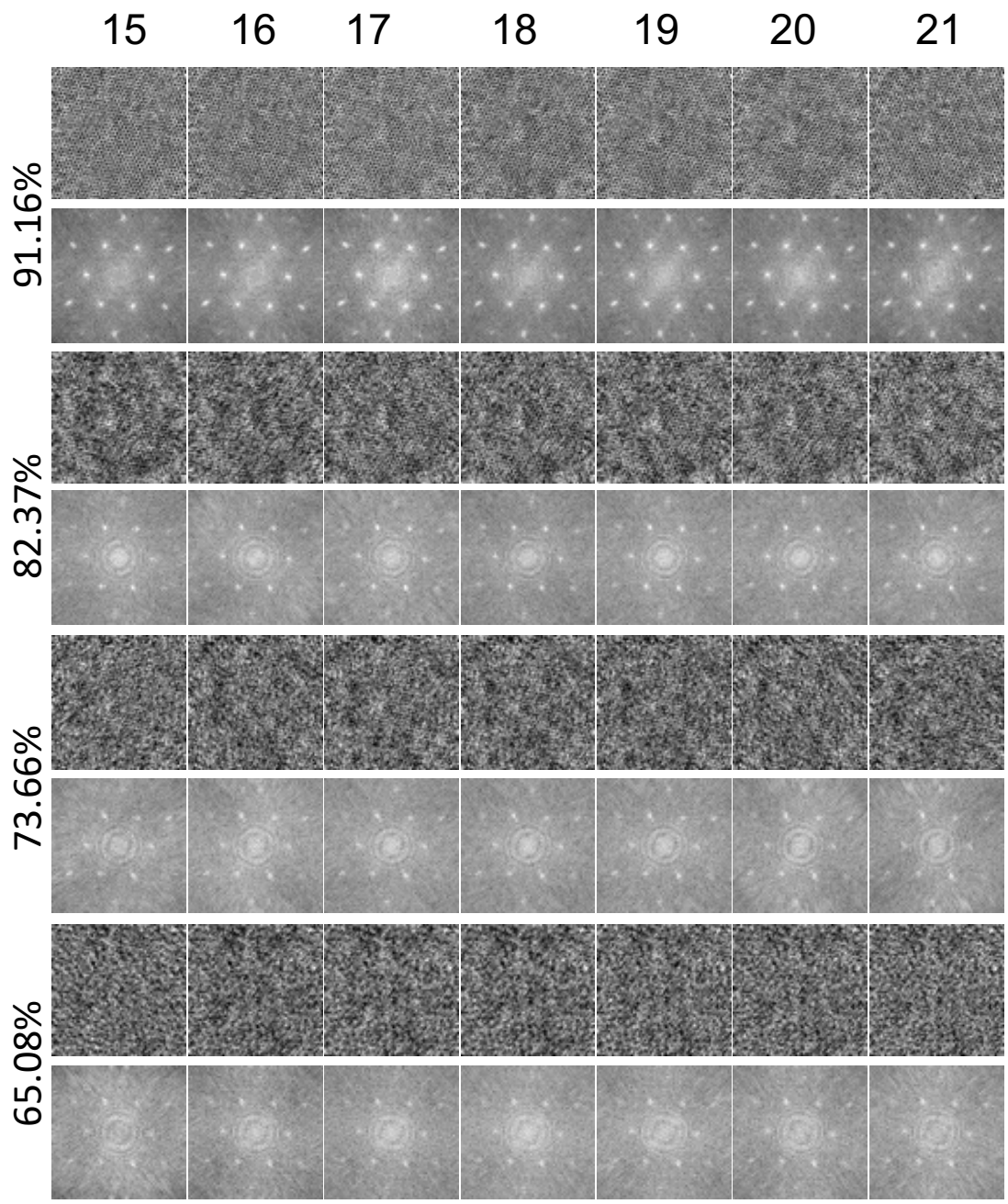

Supplementary Fig. 8

The phase images and power spectra corresponding to all resolution points evaluated under the conditions in Fig. 5b.

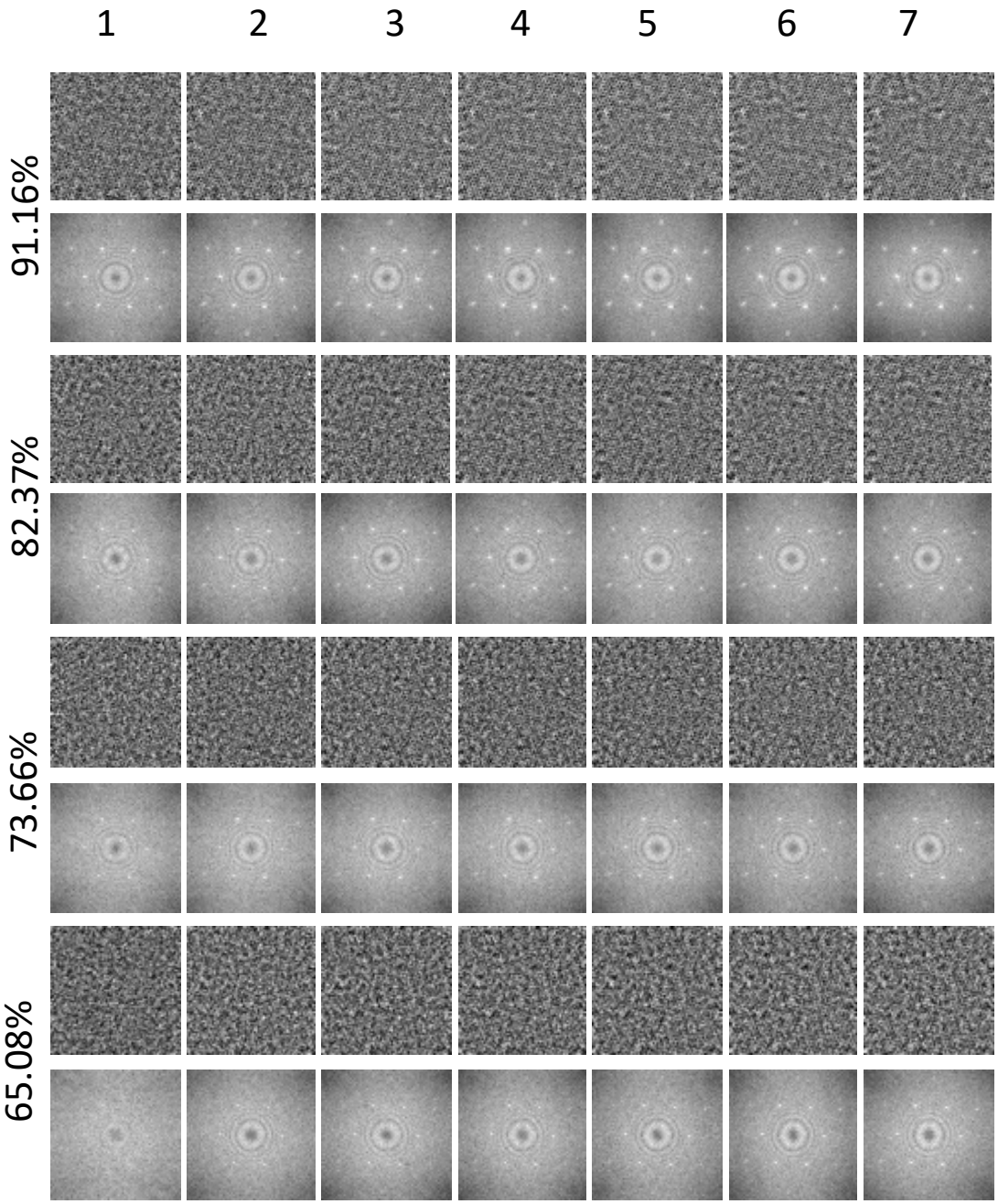
1
2
3
4
5
6
7
91.16%
82.37%
73.66%
65.08%

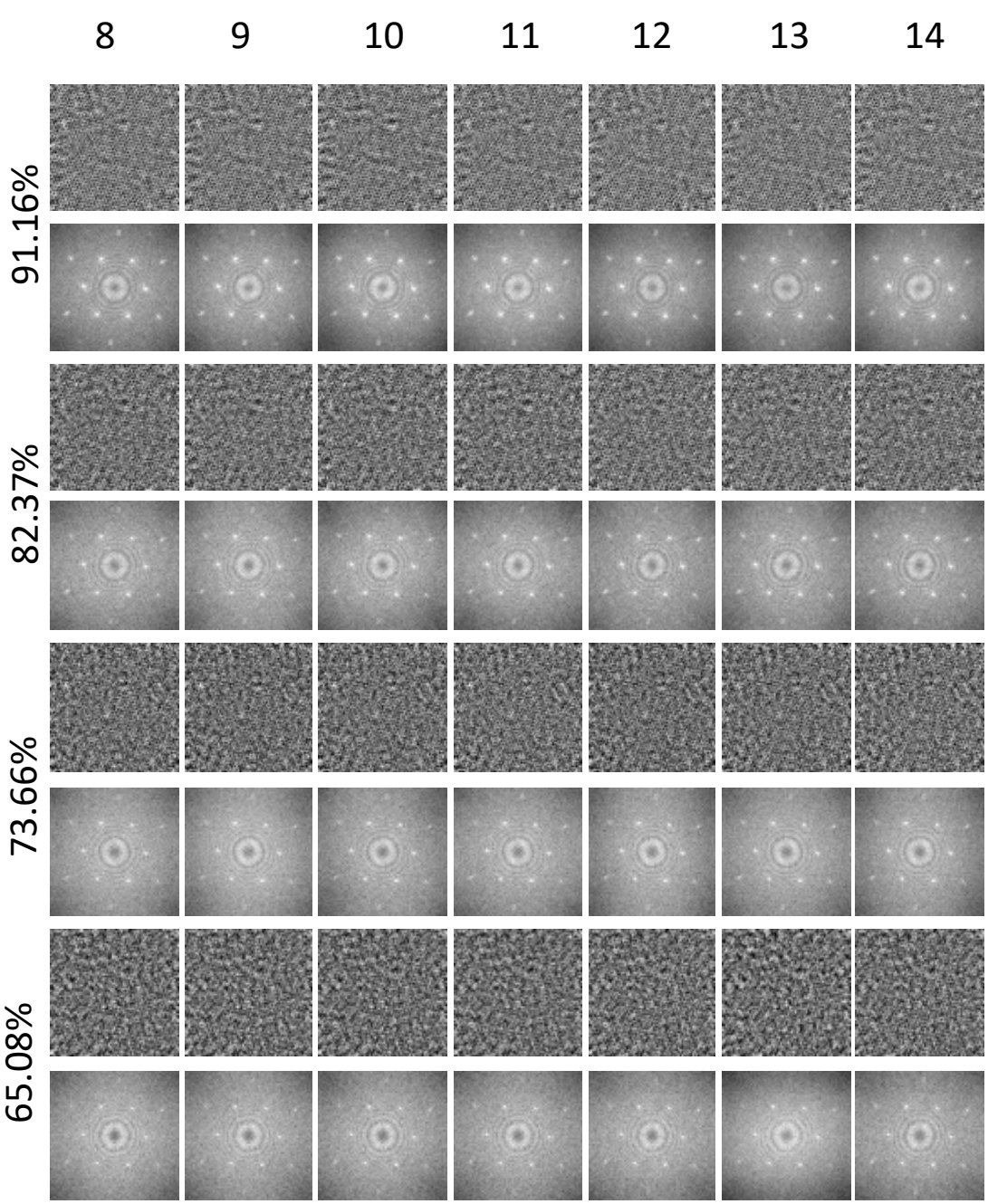
8
9
10
11
12
13
14
91.16%
82.37%
73.66%
65.08%

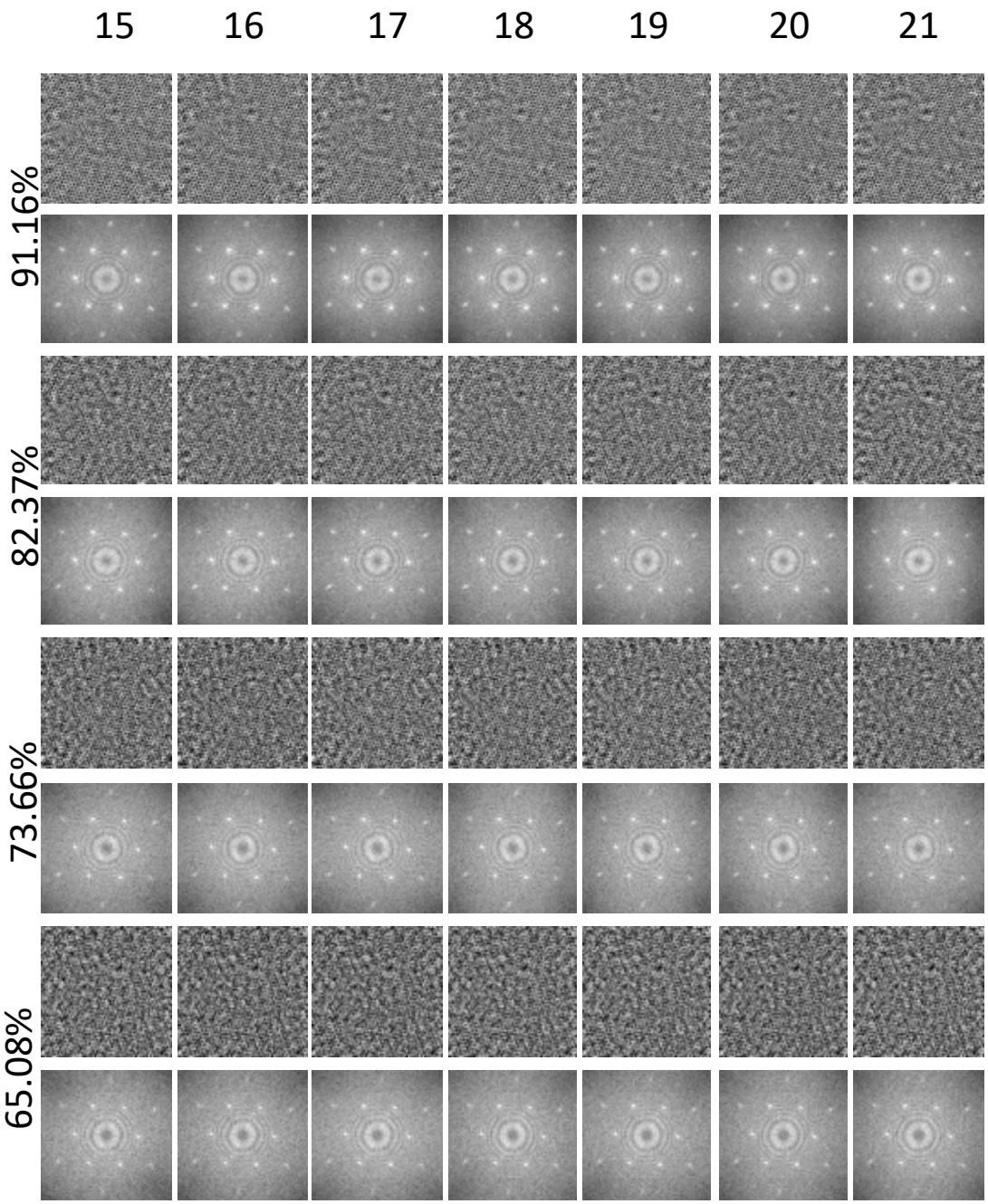

Supplementary Fig. 9

The phase images and power spectra corresponding to all resolution points evaluated under the conditions in Fig. 5c.

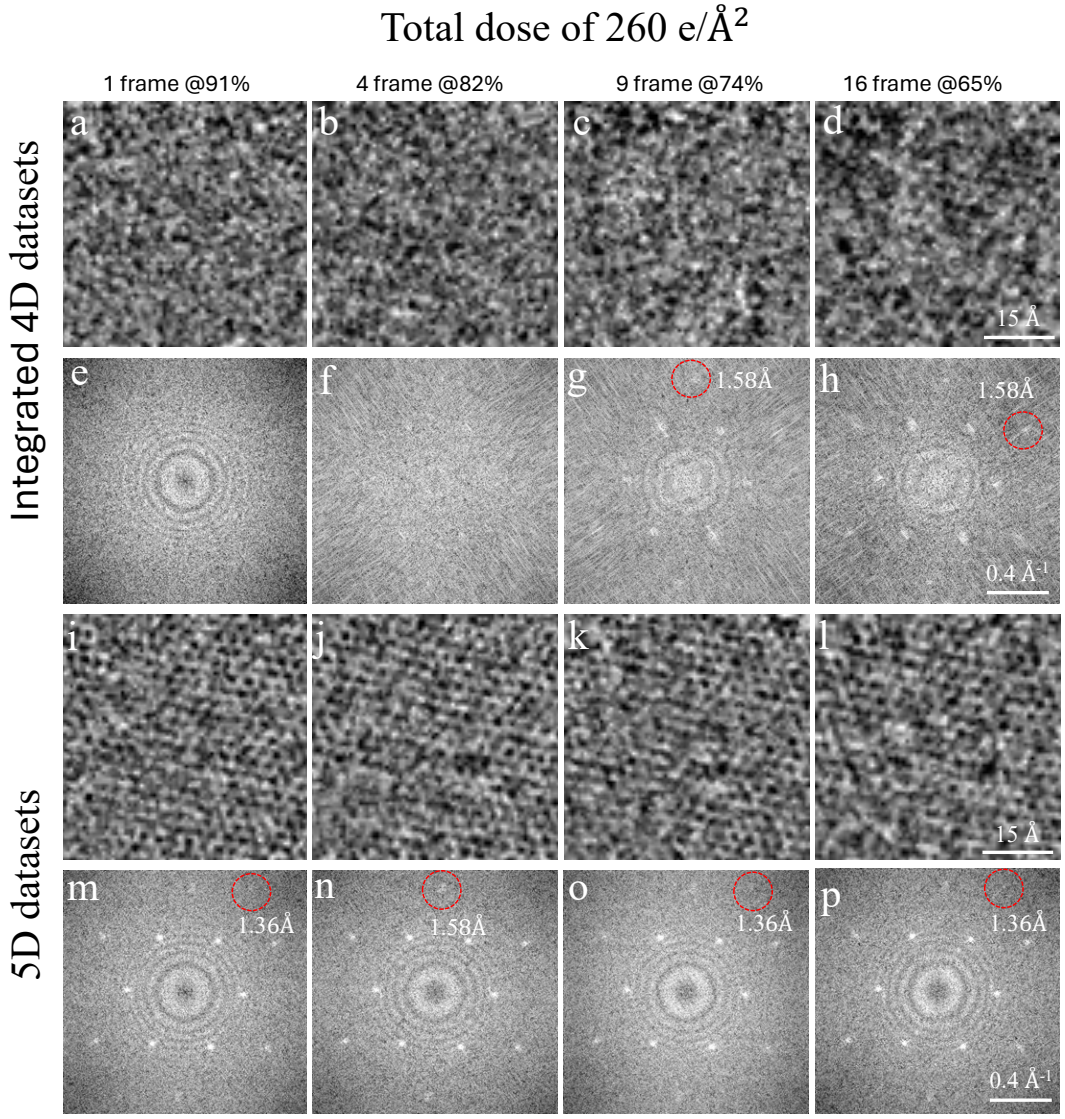

Supplementary Fig. 10

Four acquisition configurations with identical total doses of 260 e/Å² but different dose distributions corresponding, corresponding to 1, 4, 9, and 16 sub-frames and overlaps of 91%, 82%, 74%, and 65%, respectively (scan step sizes: 2.6 Å, 5.2 Å, 7.8 Å, and 10.4 Å).

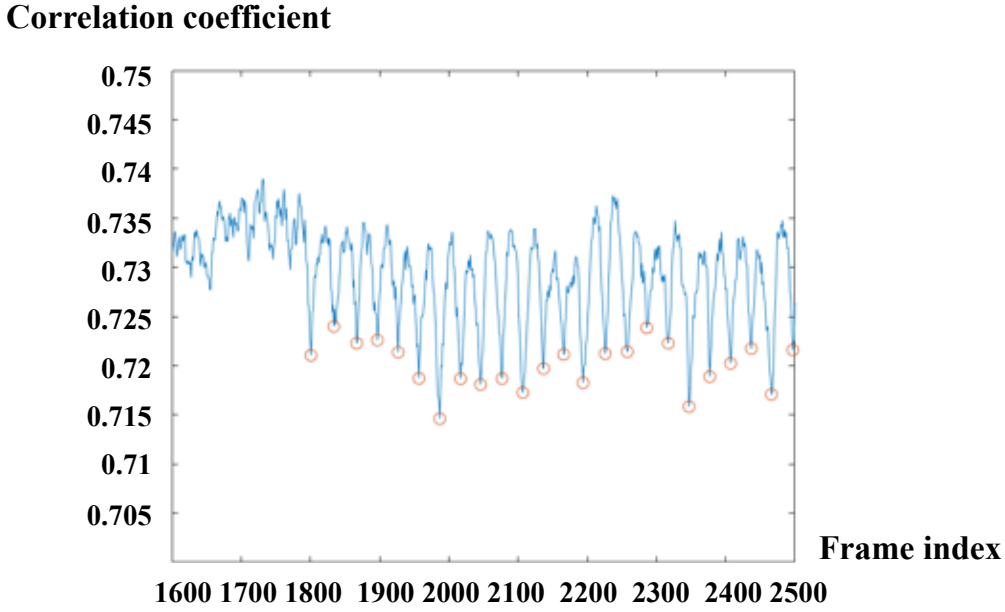

Supplementary Fig. 11

Line profile of correlation coefficients between adjacent frames for the summed diffraction patterns series F_n.

Supplementary Notes

Supplementary Note 1: Details of simulated 4D datasets and corresponding ptychographic reconstructions

4D datasets simulation

For the simulations presented in Supplementary Fig. 5, a monolayer MoS_2 molecular model was used to generate a single-slice projected potential via the atompot program developed by Kirkland et al[1]. This projected potential was subsequently converted into a transmission function using a multislice program[1]. For the 5D dataset shown in Supplementary Fig. 5, we adopted the same optical and dose parameters as in the experiments (see the Methods section in the main text for details), along with the experimentally refined probe positions.

ptychographic reconstruction

Ptychographic reconstructions shown in Supplementary Fig. 5 still adopted the ML method optimizing amplitude likelihood function to update the exit wave function and the LSQ method to update the object and probe functions. The probe was also reconstructed under a single-mode assumption and initialized identically to the probe used in the data simulation. Each reconstruction corresponding to different number of sub-frames undergoes 2000 iterations, with the first 1000 iterations performed on the integrated 4D dataset with probe position search on each integrated diffraction pattern and the other 1000 iterations performed on 5D datasets with probe position search on each sub-frame. Throughout, the object update factor and probe update factor were both set to 0.01.

Reference

1 Kirkland, E. J. in *Advanced Computing in Electron Microscopy* 157-183 (Springer US, 1998).